FEBS Letters 584 (2010) 4019–4026

FEBS Letters
journal homepage: www.FEBSLetters.org

The JNK inhibitor SP600125 enhances dihydroartemisinin-induced apoptosis by accelerating Bax translocation into mitochondria in human lung adenocarcinoma cells

Ying-Ying Lu [a], Tong-Sheng Chen [a,*], Xiao-Ping Wang [b], Jun-Le Qu [c], Min Chen [a]

[a] MOE Key Laboratory of Laser Life Science and Institute of Laser Life Science, South China Normal University, Guangzhou 510631, China
[b] Department of Anesthesiology, The First Affiliated Hospital of Jinan University, Guangzhou 510632, China
[c] Institute of Optoelectronics, Shenzhen University, Key Laboratory of Optoelectronic Devices and Systems of Ministry of Education and Guangdong Province, Shenzhen 518060, China

ARTICLE INFO

Article history:
Received 12 April 2010
Revised 13 July 2010
Accepted 10 August 2010
Available online 13 August 2010

Edited by Quan Chen

Keywords:
SP600125
Dihydroartemisinin
Apoptosis
Bax
Fluorescence recovery after photobleaching

ABSTRACT

The C-Jun N-terminal Kinase (JNK) inhibitor SP600125 is widely used to inhibit the JNK-mediated Bax activation and cell apoptosis. However, this report demonstrates that SP600125 synergistically enhances the dihydroartemisinin (DHA)-induced human lung adenocarcinoma cell apoptosis by accelerating Bax translocation and subsequent intrinsic apoptotic pathway involving mitochondrial membrane depolarization, cytochrome *c* release, caspase-9 and caspase-3 activation. The dynamical analysis of GFP-Bax mobility inside single living cells using fluorescence recovery after photobleaching revealed that SP600125 aggravated the DHA-induced decrease of Bax mobility and Bax translocation. These results for the first time present a novel pro-apoptotic action of SP600125 in DHA-induced apoptosis.

1. Introduction

Dihydroartemisinin (DHA), a semi-synthetic derivative of artemisinin, isolated from the traditional Chinese herb *Artemisia annua*, is recommended as a safe and effective mainstay in treating malaria by WHO [1]. Many recent studies have revealed that DHA can inhibit the growth of cancer cells through the apoptotic pathway [2–8]. Specifically, DHA-induced tumor cell apoptosis is implicated in the causation of G_0/G_1 cell cycle arrest [4], activation of caspases [3–6] and p38 kinase [7], decrease of Bcl-2/Bax expression ratio [4,6] and regulation of angiogenesis-related genes [8].

C-Jun N-terminal Kinase (JNK), a member of the mitogen-activated protein kinase (MAPK) family, has been implicated in the response of tumor cells to chemotherapeutic drugs [9]. It has been well established that JNK plays a critical role in death receptor-initiated extrinsic as well as mitochondrial intrinsic apoptotic pathway [9,10]. Most commonly, JNK is thought to induce mitochondria-dependent apoptosis mainly through directly or indirectly activating Bax [11–15], a pro-apoptotic Bcl-2 family member, which plays an essential role in inducing apoptosis [16]. SP600125 is an anthrapyrazole, a small molecule that acts as a reversible, ATP-competitive inhibitor of JNK1/2 [17]. Because of the specificity and effectiveness in both cultured cells and whole animals, SP600125 has become the choice of pharmacological inhibitor for assessing the role of JNK in mediating biological processes.

To explore whether JNK mediates DHA-induced Bax translocation into mitochondria and cell apoptosis, this report assesses the action of the recently described JNK inhibitor SP600125 during DHA-induced human lung adenocarcinoma (ASTC-a-1) cell apoptosis. Our data for the first time demonstrates that DHA does not activate JNK, and SP600125 enhances the DHA-induced Bax activation and cell apoptosis.

2. Materials and methods

2.1. Cell culture, transfection and treatment

Human lung adenocarcinoma ASTC-a-1 and A549 cell lines were obtained from the Department of Medicine, Jinan University

Abbreviations: DHA, dihydroartemisinin; STS, staurosporine; ROS, reactive oxygen species; JNK, c-Jun N-terminal Kinase; CCK-8, cell counting kit; FCM, Flow cytometry; FRAP, fluorescence recovery after photobleaching; $\Delta\Psi_m$, mitochondrial membrane potential; Rho123, rhodamine123; GFP-Cyt.*c*, GFP-cytochrome *c*

* Corresponding author. Fax: +86 20 85216052.
E-mail address: chentsh@scnu.edu.cn (T.-S. Chen).

0014-5793/$36.00
doi:10.1016/j.febslet.2010.08.014

(Guangzhou, China), and cultured in DMEM (GIBCO) supplemented with 10% fetal calf serum (Sijiqing, Hangzhou, China) in 5% CO_2 at 37 °C in a humidified incubator. For fluorescence experiments, cells were transiently transfected with plasmids using lipofectamine 2000 (Invitrogen, Carlsbad, CA, USA) in 35-mm dish for 24–48 h.

For every experiment described here, a lethal concentration of 20 μg/ml DHA (Bide Pharmaceutical Corporation, Guangzhou, China) based on our previous study [3] was used. Cells were pretreated with SP600125 (Sigma, St.Louis, MO, USA) for 1 h, and then incubated with DHA for indicated times.

2.2. Cell viability and apoptosis assay

Cell viability was assessed by cell counting kit (CCK-8; Dojindo Laboratories, Kumamoto, Japan) assay as previously described [3]. All experiments were performed in quadruple on three separate occasions. Cell apoptosis detection was performed by flow cytometry (FCM) analysis using Annexin V-FITC/PI apoptosis detection kit (Bender Medsystems, Vienna, Austria) as previously described [3], and for each FCM analysis 10,000 events were recorded.

2.3. Measurement of intracellular reactive oxygen species (ROS) generation

ROS generation inside living cells was measured by FCM analysis using DCFH-DA (Wako Ltd, Osaka, Japan), an oxidation-sensitive probe, which was cleaved intracellularly by non-specific esterases and turns to highly fluorescent DCF upon oxidation by ROS. For each analysis 10,000 events were recorded.

2.4. Fluorescence recovery after photobleaching (FRAP) analysis inside single living cell

To investigate the mobility of GFP-Bax after different treatments, the GFP in the indicating regions of living cells were photobleached by scanning the region with the maximal 488 nm laser line, and subsequent the entire cell was imaged at every 5 s with a low laser power (5% power) excitation for a duration of 500 s to monitor the recovery of fluorescence.

2.5. Detection of Bax translocation and cytochrome c release

A confocal laser scanning microscope (LSM510/ConfoCor2, Zeiss, Jena, Germany) was used to perform fluorescence imaging of Bax translocation and cytochrome *c* release inside single living cells. Images of cells co-expressing GFP-Bax or GFP-cytochrome *c* (GFP-Cyt.*c*) and DsRed-Mito were collected using dual fluorescence channels. The excitation wavelengths were 488 nm for GFP and 543 nm for DsRed. The emission fluorescence channels were 500–550 nm for GFP and 600–650 nm for DsRed.

2.6. Measurement of mitochondrial membrane potential ($\Delta\Psi_m$)

Rhodamine123 (Rho123; Sigma), a potential-sensitive dye, was used to evaluate changes in $\Delta\Psi_m$ by FCM as previously described [3]. Results were expressed as the proportion of cells with lost or low $\Delta\Psi_m$ which was estimated by reduced fluorescence intensity from Rho123, and for each analysis 10,000 events were recorded.

2.7. Fluorometric assay for caspase activity

Activities of caspase-9 and -3 were measured using fluorogenic substrates Ac-LEHD-AFC and Ac-DEVD-AFC (Alexis Biochemicals, Lausen, Switzerland) as previously described [3]. Caspase activity was measured continuously by monitoring the release of fluorigenic AFC using auto microplate reader (infinite M200, Tecan, Austria). Caspase-like activity was reported as the ratio of the fluorescence output in treated samples relative to untreated controls.

2.8. Western blot analysis

Preparation of whole cell lysates and Western blot were carried out as previously described [3]. Anti-phospho-JNK, anti-JNK, anti-β-actin, anti-Bax, and anti-Cox IV antibodies were obtained from Cell Signaling (Beverly, MA, USA). Anti-cytochrome *c* antibody was obtained from Santa Cruz Biotechnology (Santa Cruz, CA). IR-Dye Rdye® 800CW anti-rabbit IgG and Alexa Fluor 680® goat anti-Mouse IgG were purchased from Molecular Probes (Eugene, OR, USA). Detection was performed using the Odyssey Scanning Infrared Fluorescence Imaging System (LI-COR, USA).

2.9. Statistics analysis

Results were expressed as mean ± standard deviation (S.D.). Differences between groups were compared using Student's *t*-test by SPSS software. Significance was defined as $P < 0.05$.

3. Results

3.1. SP600125 pretreatment enhanced DHA-induced cell apoptosis

We found that SP600125 treatment alone did not affect cell growth, whereas pretreating ASTC-a-1 cells with 10 or 20 μM SP600125 significantly increased DHA-induced cell cytotoxicity (Fig. 1A). Meanwhile, cells were treated with DHA for 0, 12 and 24 h in the absence or presence of 0.5 and 1 μl DMSO which were equivalent to that in 10 and 20 μM SP600125, respectively. In order to avoid the vehicle (DMSO) response, 10 μM of SP600125 was selected for every experiment without indicated concentration in this report. Also, the augment of SP600125 on DHA-induced cell death was observed in A549 cell line (Fig. 1B). However, SP600125 did not have a similar effect on Staurosporine (STS; Alexis Biochemicals, Lausen, Switzerland) -induced cell death (Fig. 1C), suggesting a specific role of SP600125 in conjunction with DHA.

To determine whether SP600125 enhanced the DHA-induced cell death through accelerating apoptosis, the early apoptotic characteristic of phosphatidyl serine (PS) externalization was quantified by annexin V/PI staining. As shown in Fig. 1D, the percentage of apoptosis in ASTC-a-1 cells cotreated with DHA and SP600125 (45.6%) was significantly higher than that in cells exposed to DHA (29.3%) or SP600125 (3.3%) alone, indicating a potential synergistic effect of SP600125 on cell apoptosis. ASTC-a-1 cell line was selected for every experiment without indication in this report.

3.2. DHA did not activate JNK pathway

Firstly, anisomycin (Alexis Biochemicals, Lausen, Switzerland), a well-known JNK activator, was used to investigate whether JNK could be activated and SP600125 acted as a JNK inhibitor. As shown in Fig. 2A and B, our results showed that treating cells with 1 or 1.5 μg/ml anisomycin for 2 h significantly induced the phosphorylation of JNK, whereas SP600125 pretreatment markedly blocked JNK phosphorylation, in which DHA did not influence the inhibitory effect of SP600125 on JNK phosphorylation.

Next, to assess whether JNK was involved in the DHA-induced apoptosis, we detected the JNK phosphorylation at 0, 6, 12 and 24 h after DHA treatment. As shown in Fig. 2C, in contrast to anisomycin treatment, although DHA treatment did not activate JNK, we noticed that treating cells with DHA for 12 or 24 h not 6 h induced

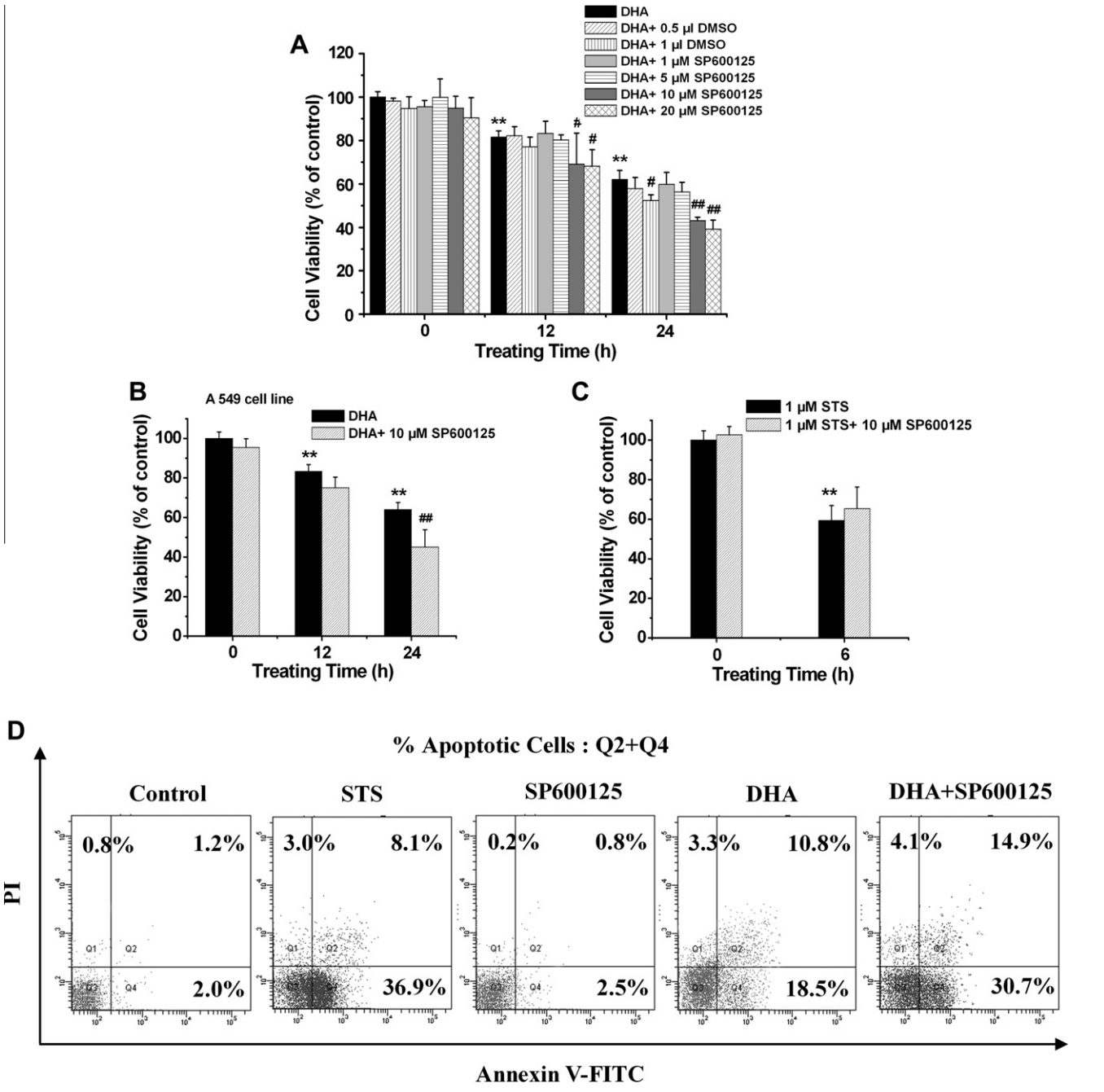

Fig. 1. SP600125 pretreatment enhanced DHA-induced ASTC-a-1 cell apoptosis. (A) Effect of SP600125 pretreatment on DHA-induced cytotoxicity by CCK-8. Cells were treated with 20 μg/ml DHA for 0, 12 and 24 h in the presence or absence of DMSO and 1, 5, 10 or 20 μM SP600125, respectively. $^{**}P < 0.01$, compared with control; $^{\#}P < 0.05$, $^{\#\#}P < 0.01$, compared with DHA treatment alone. (B) Effect of SP600125 pretreatment on DHA-induced cytotoxicity by CCK-8 in A549 cells. Cells were treated with 20 μg/ml of DHA for 0, 12 and 24 h in the presence or absence of 10 μM SP600125. $^{**}P < 0.01$, compared with control; $^{\#\#}P < 0.01$, compared with DHA treatment alone. (C) Effect of SP600125 pretreatment on STS-induced cytotoxicity by CCK-8. Cells were treated with 1 μM STS for 0 and 6 h in the presence or absence of 10 μM SP600125, respectively. $^{**}P < 0.01$, compared with control. (D) FCM analysis of apoptosis of cells upon different treatments. Cells were treated with DHA for 0 and 24 h with or without the addition of SP600125 and then stained with Annexin V-FITC/PI before being analyzed by FCM. STS-treated cells were used as a positive control.

a reduction in JNK expression level, which was blocked by pretreatment of Z-VAD-fmk, a broad spectrum caspase inhibitor. These results implied that the significant decrease of JNK protein level in response to DHA treatment was possibly due to cell death.

3.3. SP600125 pretreatment attenuated DHA-elicited ROS generation

We found that N-acetyl cysteine (NAC; Sigma), a ROS scavenger, significantly inhibited the DHA-induced cytotoxicity (Fig. S1), demonstrating that DHA-elicited ROS, mostly due to the reaction of endoperoxide bridge of DHA with heme irons [18], mediated the DHA-induced apoptosis. To determine the effect of SP600125 on DHA-elicited ROS, we used DCFH-DA to detect the ROS level inside living cells. Results from FCM analysis (Fig. 2D) consistently demonstrated that DHA treatment induced a rapid increase in DCF fluorescence, which was remarkably attenuated by SP600125 pretreatment, indicating that the synergistic effect of SP600125 on DHA-induced apoptosis was not owing to promoting the DHA-elicited ROS generation.

3.4. SP600125 pretreatment aggravated the decrease of Bax mobility by DHA

Here, we used FRAP technique to assess Bax mobility inside single living cells showing even distribution of GFP-Bax in cytoplasm during DHA-induced apoptosis. We noticed a rapid refilling of GFP-Bax in the photobleached area for control cell (Fig. 3A: control) as well as the cells treated with SP600125 alone (Fig. 3A: SP600125), confirming that GFP-Bax is a soluble protein with high mobility in untreated cells. However, DHA treatment induced a slow refilling of GFP-Bax in the photobleached area (Fig. 3A: DHA), which might be due to both the Bax conformational change and partially binding to certain organelles. Strikingly, co-treating cells with SP600125 and DHA almost blocked the fluorescence recovery in the photobleached area (Fig. 3A: DHA + SP600125). Fig. 3B showed the dynamics of FRAP from 50 to 60 cells in three independent experiments for control, SP600125-treated, DHA-treated, DHA- and SP600125-cotreated cells. These results suggested that SP600125 pretreatment significantly aggravated the DHA-induced decrease of Bax mobility, which might be due to the conformational change and oligomerization of Bax before the formation of Bax clusters.

3.5. SP600125 pretreatment promoted DHA-induced Bax translocation into mitochondria

In contrast to control cells (Fig. 3A: control), co-treating cells with SP600125 and DHA induced Bax clusters formation, in which the fluorescence recovery in the photobleached area was completely blocked (Fig. 3C), which was consistent with the dynamics of FRAP from 50 to 60 cells in three independent experiments shown in Fig. 3D. These results demonstrated that Bax irreversibly

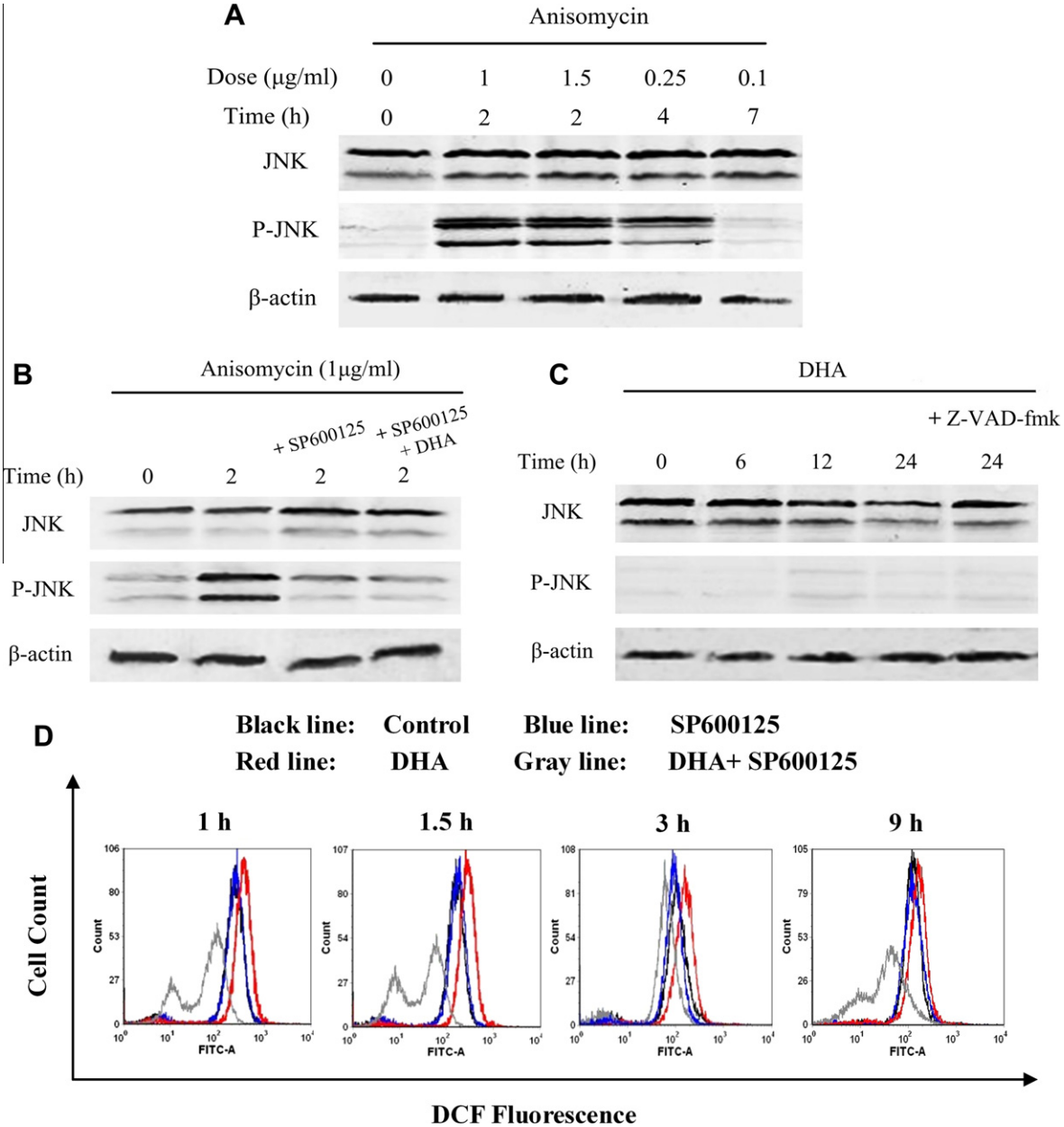

Fig. 2. DHA did not activate JNK pathway and SP600125 pretreatment attenuated DHA-elicited ROS generation. (A–C) Soluble protein extracts obtained from cells under indicated treatments were analyzed by Western blot with anti-phospho-JNK, anti-JNK, β-actin antibodies, respectively. Anisomycin treatment was used as a positive control. (D) FCM analysis of ROS generation. Untreated or treated cells were harvested and stained with 20 μM DCFH-DA for 30 min in the dark before being analyzed by FCM.

localized to certain organelle membranes such as mitochondria or endoplasmic reticulum during apoptosis induced by SP600125 and DHA cotreatment.

Next, we used confocal fluorescence microscopy to image the spatial distribution of Bax and mitochondria inside single living cells co-expressing GFP-Bax and DsRed-Mito. We found that co-treatment with DHA and SP600125 induced Bax translocation into mitochondria as revealed by the overlaps of GFP-Bax and DsRed-Mito (Fig. 3E). Statistical results from 300 cells in three independent experiments (Fig. 3F) showed that at 24 h after DHA

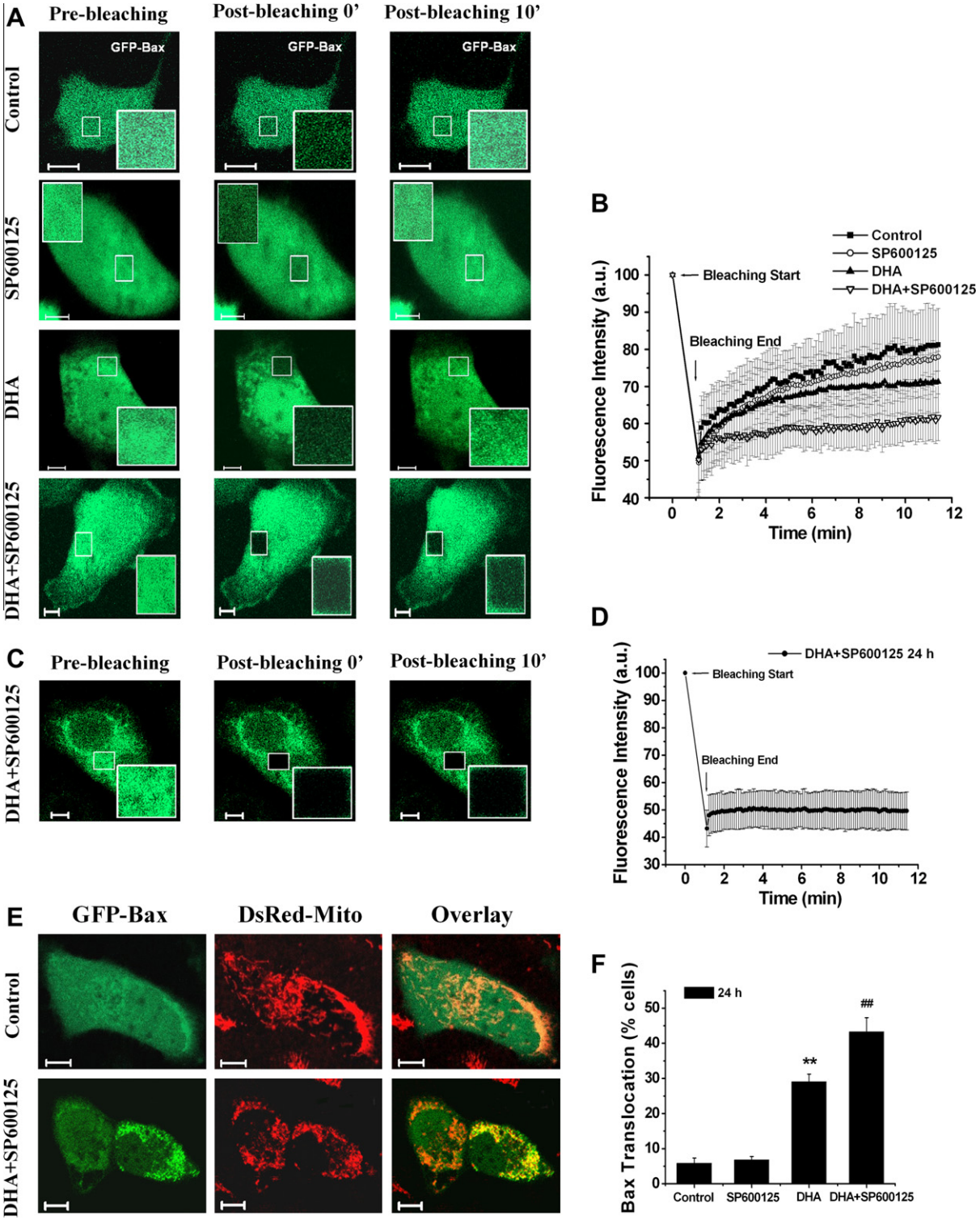

Fig. 3. SP600125 pretreatment aggravated the decrease of Bax mobility by DHA and promoted the DHA-induced Bax translocation into mitochondria. (A) Typical time-lapse imaging of the mobility of GFP-Bax during photobleaching under different treatments. Scale Bar: 5 μm. (B) Dynamics of FRAP from 50 to 60 cells in three independent experiments for each condition. (C) Typical time-lapse imaging of the mobility of GFP-Bax during photobleaching in cells showing Bax clusters under SP600125 pretreatment. Scale Bar: 5 μm. (D) Dynamics of FRAP inside living cells from 50 to 60 cells in three independent experiments for DHA and SP600125-cotreated cells. (E) Typical fluorescence images of the spatial distribution of Bax and mitochondria inside single living cells co-expressing GFP-Bax and DsRed-Mito. Scale Bar: 20 μm. (F) Quantification of cells showing GFP-Bax translocation. Cells were treated with DHA for 0 and 24 h in the presence or absence of SP600125. Data were obtained from 300 cells in three independent experiments. $^{**}P < 0.01$, compared with control; $^{\#\#}P < 0.01$, compared with DHA treatment alone.

treatment, the percentage of cells showing Bax translocation into mitochondria increased from 4.85 ± 1.5% (control cells) to 29 ± 2.1%, which was raised to 43.25 ± 4.05% in the presence of SP600125, suggesting that SP600125 enhanced the DHA-induced apoptosis by promoting the DHA-induced Bax translocation into mitochondria.

3.6. SP600125 pretreatment promoted DHA-induced mitochondrial apoptotic pathway

Firstly, we used FCM to evaluate the mitochondrial membrane depolarization indicating the loss of $\Delta\Psi_m$ by measuring the fluorescence of Rho123 under various treatments. At 12 and 24 h after DHA treatment, the percentage of cells with lost or low Rho123 fluorescence intensity were 14.2% and 30.3%, which increased to 20.7% and 45.1% in the case of SP600125 pretreatment, respectively (Fig. 4A), indicating that SP600125 pretreatment promoted the DHA-induced mitochondrial membrane depolarization.

Secondly, the release of cytochrome *c* was investigated in single living cells co-expressing GFP-Cyt.*c* and DsRed-Mito using time-lapse confocal fluorescence microscopy. As shown in Fig. 4B, GFP-Cyt.*c* completely localized on mitochondria (DsRed-Mito) in control cell (upper panel), while DHA induced cytochrome *c* release (middle panel), and SP600125 aggravated the DHA-induced cytochrome c release (lower panel). Statistical results from 300 cells in three independent experiments (Fig. 4C) showed that at 24 h after DHA treatment, the percentage of cells showing cytochrome *c* release was increased from 6.1 ± 2.02% (control) to 31.8 ± 6.13%,

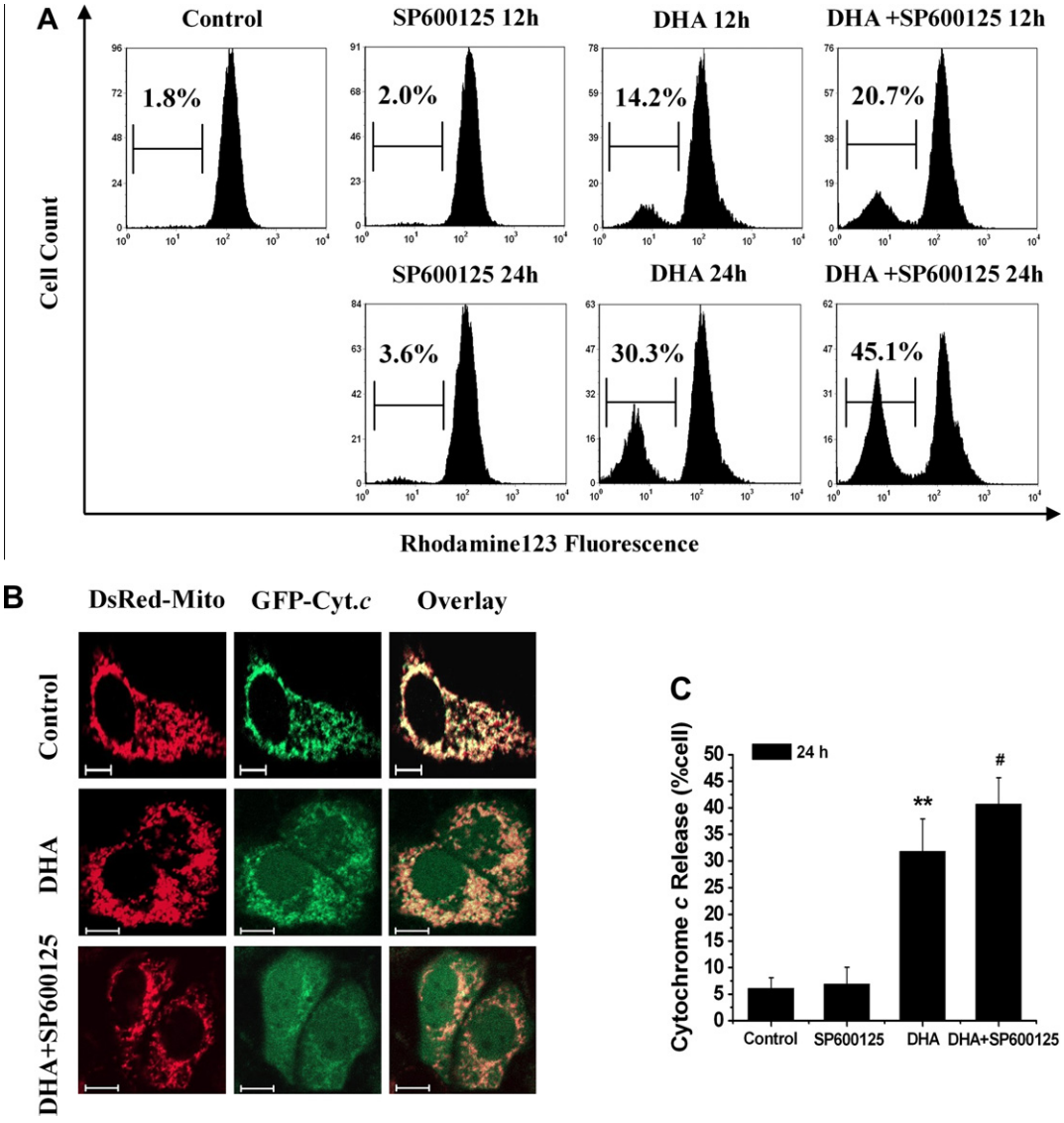

Fig. 4. SP600125 pretreatment promoted the DHA-induced mitochondrial membrane depolarization, cytochrome *c* release, subsequently caspase-9 and caspase-3 activation. (A) FCM analysis of the loss of $\Delta\Psi_m$ upon different treatments. Cells were treated with DHA for 0, 12 and 24 h in the presence or absence of SP600125 and then stained with Rho123 before being analyzed by FCM. (B) Typical fluorescence images of cytochrome *c* release in living cells under different treatments. Scale Bar: 5 μm. (C) Quantification of cells showing cytochrome *c* release. Data were obtained from 300 cells in three independent experiments. $^{**}P < 0.01$, compared with control; $^{\#}P < 0.05$, compared with DHA treatment alone. (D) Western blot analysis of Bax translocation and cytochrome *c* release. Cells were treated with DHA for 24 h in the presence or absence of SP600125. The cytosolic and mitochondrial proteins were extracted using a mitochondria/cytosol fractionation kit and then analyzed by Western blot using antibodies against Bax, Cyt.*c*, Cox IV and β-actin. (E, F) Detection of caspase-9 and caspase-3 activation by fluorometric assay. Cells were treated with DHA for 0 and 24 h with or without SP600125, and STS-treated cells were used as a positive control. Caspase activity was measured using the fluorescence substrate as described in Section 2, and the activation index was determined as the ratio between the activity in extracts of treated cells to that measured in extracts of control cells. Data were analyzed with SPSS10.0 software in three independent experiments. $^{**}P < 0.01$, compared with control; $^{\#}P < 0.05$, $^{\#\#}P < 0.01$, compared with DHA treatment alone.

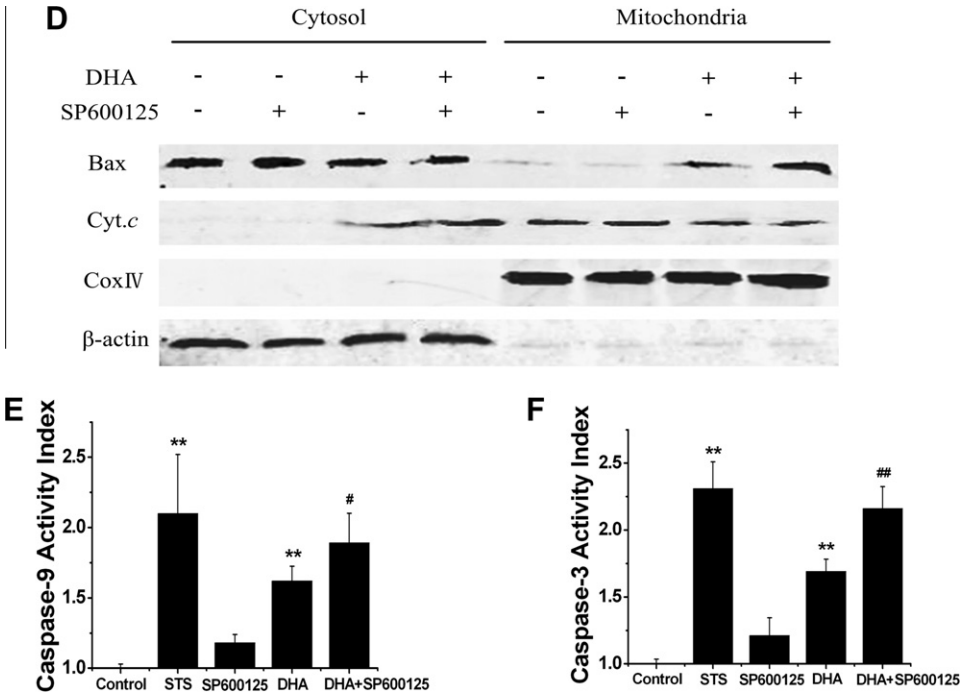

Fig. 4 (*continued*)

which was raised to 40.7 ± 4.95% in the presence of SP600125. Also, western blot analysis further confirmed that SP600125 pretreatment enhanced the DHA-induced cytochrome *c* release as well as the translocation of Bax into mitochondria (Fig. 4D).

Thirdly, the activation of caspase-9 was evaluated by determining fluorogenic AFC release. Ac-LEHD-AFC, which can be cleaved by caspase-9-like proteases, was associated with caspase-9 activation. STS-treated cells were used as a positive control. As can be seen in Fig. 4E, DHA induced a nearly 1.6-fold increase of caspase-9 activity compared with control, while co-treatment with SP600125 and DHA modestly enhanced the caspase-9 activity compared with DHA treatment alone, indicating that SP600125 pretreatment enhanced the DHA-induced caspase-9 activation. Likewise, the activation of caspase-3 was also evaluated by determining fluorogenic AFC release. As can be seen in Fig. 4F, DHA induced a nearly 1.7-fold increase of caspase-3 activity compared with control, while co-treatment with SP600125 and DHA significantly enhanced the caspase-3 activity compared with DHA treatment alone, suggesting that SP600125 pretreatment enhanced the DHA-induced caspase-3 activation.

Collectively, these results revealed that SP600125 pretreatment promoted the DHA-induced mitochondrial membrane depolarization, cytochrome c release, and subsequent caspase-9 and caspase-3 activation.

4. Discussion

SP600125 is widely and commonly used for assessing the complex roles of JNK in mediating biological processes [17]. However, in our experimental system, SP600125 is not functioning as a simple JNK inhibitor, which supports a novel pro-apoptotic role for SP600125 in conjunction with DHA and encourages us to verify its underlying mechanism.

ROS, recommended as important mediators for apoptotic signaling pathway, are thought to be associated with a number of human diseases, especially cancer [19]. A burst of exogenous ROS generation has been observed in DHA-induced apoptosis [5], which is mostly due to the reaction of endoperoxide bridge of DHA with heme irons [18]. The present study showed that SP600125 pretreatment did not promote, but markedly attenuated the DHA-induced ROS burst (Fig. 2D). Accordingly, it is possible that ROS over-scavenging lead to cell apoptosis.

Mostly, JNK mediates Bax activation and translocation, and these events can be significantly blocked by SP600125 [11]. However, in our system, SP600125 pretreatment enhances the DHA-induced Bax activation and translocation into mitochondria (Fig. 3), which may be responsible largely for the synergistic effect of this combination treatment. It has been reported that Mcl-1, an anti-apoptotic member of the Bcl-2 family, inhibits Bax activation and translocation into mitochondria independent of an interaction between these two proteins [20]. Therefore, we assessed the effect of Mcl-1 on the augment of SP600125 in the DHA-induced apoptosis (Fig. S2). Our results showed that silencing Mcl-1 by transfection of shMcl-1-980 or shMcl-1-1039 both markably decreased the cell viability either in DHA-treated or DHA and SP600125-cotreated cells compared with the cells without shMcl-1 transfection. However, transfection of shMcl-1 caused no significant difference in cell viability between DHA-treated and DHA and SP600125-cotreated cells, implying that the function of Mcl-1 was not responsible for the synergistic effect of SP600125 on DHA-induced apoptosis. Additionally, we found that the overexpression of Bcl-xL, an another anti-apoptotic members of Bcl-2 family, prevented DHA-induced Bax translocation (data not shown). Therefore, our further studies would focus on the confirmation of the action of Bcl-xL, Mcl-1 or other mediators in DHA/SP600125-induced apoptosis.

Our present findings demonstrate that SP600125 pretreatment enhances DHA-induced apoptosis mainly through a mitochondrial apoptotic pathway involving mitochondrial membrane depolarization, cytochrome c release, and subsequent caspase-9 and caspase-3 activation. Moreover, one point worthy to be mentioned was that SP600125 pretreatment remarkably promoted caspase-3 activation (Fig. 4F), but modestly enhanced the cytochrome c release and caspase-9 activation (Fig. 4B–E). It is therefore possible that SP600125 pretreatment induce the release of other mitochondrial apoptotic factors, such as Smac/DIABLO, which activate caspase-3 by blocking the inhibitors of apoptosis (IAPs) [21].

In conclusion, our present study supports a novel pro-apoptotic role for SP600125 in conjunction with DHA. This is the first report that SP600125 synergistically enhances the DHA-induced ASTC-a-1 cell apoptosis by accelerating Bax translocation and subsequent mitochondrial apoptotic pathway.

Acknowledgements

This study was supported by the Program for Changjiang Scholars and Innovative Research Team in University (Grant No. IRT0829), and the Natural Science Foundation of China (Grant No. 310712189 and 81071491).

Appendix A. Supplementary data

Supplementary data associated with this article can be found, in the online version, at doi:10.1016/j.febslet.2010.08.014.

References

[1] Haynes, R.K. (2001) Artemisinin and derivatives: the future for malaria treatment. Curr. Opin. Infect. Dis. 14, 719–726.
[2] Singh, N.P. and Lai, H.C. (2004) Artemisinin induces apoptosis in human cancer cells. Anticancer Res. 24, 2277–2280.
[3] Lu, Y.Y., Chen, T.S., Qu, J.L., Pan, W.L., Sun, L. and Wei, X.B. (2009) Dihydroartemisinin (DHA) induces caspase-3-dependent apoptosis in human lung adenocarcinoma ASTC-a-1 cells. J. Biomed. Sci. 16, 16.
[4] Hou, J., Wang, D., Zhang, R. and Wang, H. (2008) Experimental therapy of hepatoma with artemisinin and its derivatives: in vitro and in vivo activity, chemosensitization and mechanisms of action. Clin. Cancer Res. 14, 5519–5530.
[5] Disbrow, G.L., Baege, A.C., Kierpiec, K.A., Yuan, H., Centeno, J.A., Thibodeaux, C.A., Hartmann, D. and Schlegel, R. (2005) Dihydroartemisinin is cytotoxic to papillomavirus expressing epithelial cells in vitro and in vivo. Cancer Res. 65, 10854–10861.
[6] Chen, T., Li, M., Zhang, R.W. and Wang, H. (2009) Dihydroartemisinin induces apoptosis and sensitizes human ovarian cancer cells to carboplatin therapy. J. Cell Mol. Med. 13, 1358–1370.
[7] Lu, J.J., Meng, L.H., Cai, Y.J., Chen, Q., Tong, L.J., Lin, L.P. and Ding, J. (2008) Dihydroartemisinin induces apoptosis in HL-60 leukemia cells dependent of iron and p38 mitogen-activated protein kinase activation but independent of reactive oxygen species. Cancer Biol. Ther. 7, 1017–1023.
[8] Lee, J., Zhou, H.J. and Wu, X.H. (2006) Dihydroartemisinin downregulates vascular endothelial growth factor (VEGF) expression and induces apoptosis in chronic myeloid leukemia K562 cells. Cancer Chemother. Pharmacol. 57, 213–220.
[9] Dhanasekaran, D.N. and Reddy, E.P. (2008) JNK signaling in apoptosis. Oncogene 27, 6245–6251.
[10] Papadakis, E.S., Finegan, K.G., Wang, X., Robinson, A.C., Guo, C., Kayahara, M. and Tournier, C. (2006) The regulation of Bax by c-Jun N-terminal protein kinase (JNK) is a prerequisite to the mitochondrial-induced apoptotic pathway. FEBS Lett. 580, 1320–1326.
[11] Kim, B.J., Ryu, S.W. and Song, B.J. (2006) JNK- and p38 kinase-mediated phosphorylation of Bax leads to its activation and mitochondrial translocation and to apoptosis of human hepatoma HepG2 cells. J. Biol. Chem. 281, 21256–21265.
[12] Lei, K. and Davis, R.J. (2003) JNK phosphorylation of Bim-related members of the Bcl-2 family induces Bax-dependent apoptosis. Proc. Natl. Acad. Sci. 100, 2434–2437.
[13] Tsuruta, F., Sunayama, J., Mori, Y., Hattori, S., Shimizu, S., Tsujimoto, Y., Yoshioka, K., Masuyama, N. and Gotoh, Y. (2004) JNK promotes Bax translocation to mitochondria through phosphorylation of 14-3-3 proteins. EMBO J. 23, 1889–1899.
[14] Zhang, L., Xing, D., Liu, L., Gao, X. and Chen, M. (2007) TNF alpha induces apoptosis through JNK/Bax-dependent pathway in differentiated, but not naive PC12 cells. Cell Cycle 12, 1479–1486.
[15] Keramaris, E., Ruzhynsky, V.A., Callaghan, S.M., Wong, E., Davis, R.J., Flavell, R., Slack, R.S. and Park, D.S. (2008) Required roles of Bax and JNKs in central and peripheral nervous system death of retinoblastoma-deficient mice. J. Biol. Chem. 283, 405–415.
[16] Wei, M.C., Zong, W.X., Cheng, E.H., Lindsten, T., Panoutsakopoulou, V., Ross, A.J., Roth, K.A., MacGregor, G.R., Thompson, C.B. and Korsmeyer, S.J. (2001) Proapoptotic BAX and BAK: a requisite gateway to mitochondrial dysfunction and death. Science 292, 727–730.
[17] Bennett, B.L., Sasaki, D.T., Murray, B.W., O'Leary, E.C., Sakata, S.T., Xu, W., Leisten, J.C., Motiwala, A., Pierce, S. and Satoh, Y. (2001) SP600125, an anthrapyrazolone inhibitor of Jun N-terminal kinase. Proc. Natl. Acad. Sci. 98, 13681–13686.
[18] Li, P.C., Lam, E., Roos, W.P., Zdzienicka, M.Z., Kaina, B. and Efferth, T. (2008) Artesunate derived from traditional Chinese medicine induces DNA damage and repair. Cancer Res. 68, 4347–4351.
[19] Benhar, M., Engelberg, D. and Levitzki, A. (2002) ROS, stress-activated kinases and stress signaling in cancer. EMBO Rep. 3, 420–425.
[20] Germain, M., Milburn, J. and Duronio, V. (2008) MCL-1 inhibits BAX in the absence of MCL-1/BAX interaction. J. Biol. Chem. 283, 6384–6392.
[21] Verhagen, A.M., Ekert, P.G., Pakusch, M., Silke, J., Connolly, L.M., Reid, G.E., Moritz, R.L., Simpson, R.J. and Vaux, D.L. (2000) Identification of DIABLO, a mammalian protein that promotes apoptosis by binding to and antagonizing IAP proteins. Cell 102, 43–53.